European Journal of Remote Sensing - 2015, 48: 383-401
doi: 10.5721/EuJRS20154822
Received 15/05/2015, accepted 04/08/2015

European Journal of Remote Sensing
An official journal of the Italian Society of Remote Sensing

www.aitjournal.com

Assessment of three algorithms for the operational estimation of [CHL] from MODIS data in the Western Mediterranean Sea

Maurizio Pieri[1,2]*, Luca Massi[3], Luigi Lazzara[3], Caterina Nuccio[3], Chiara Lapucci[1,2] and Fabio Maselli[2]

[1]IBIMET-CNR, Via Madonna del Piano 10, 50019 Sesto Fiorentino (Fi), Italy
[2]LaMMA Consortium, Via Madonna del Piano 10, 50019 Sesto Fiorentino (Fi), Italy
[3]Dipartimento di Biologia, Università di Firenze, Via Micheli 1, 50121 Firenze, Italy
*Corresponding author, e-mail address: pieri@lamma.rete.toscana.it

Abstract

Three algorithms based on MODIS imagery were evaluated for the estimation of Chlorophyll-a concentration ([CHL]) in the Western Mediterranean Sea. The first algorithm (OC3M) is usually applied at global scale, while the second (MedOC3), has been used in the Mediterranean basin. The third algorithm (SAM_LT), specifically developed for the Ligurian and North Tyrrhenian Seas, is here described and applied, in its updated version. The three algorithms were assessed through comparison with 240 sea [CHL] samples collected during the 2002-2011 decade. The results obtained show that OC3M is the most accurate algorithm when used for the entire Western Mediterranean, but is outperformed by SAM_LT in the area where this was originally developed. The impact of different MODIS quality flags on the three algorithms has been finally evaluated, providing guidelines for their operational application in the study area.

Keywords: Ocean color, chlorophyll-a, remote sensing reflectance, MODIS, flags, western Mediterranean.

Introduction

Satellite remote sensing observations of ocean color are crucial for understanding marine biology and evaluating the impacts of global warming scenarios. Seawater color is partly related to phytoplankton pigments, which, through the photosynthesis process, provides most of primary production in the aquatic food web. Phytoplankton also controls the carbon dioxide uptake by the oceans (biological pump) and, therefore, plays a key role in the global carbon cycle [Alvain et al., 2011; Gregg and Rousseaux, 2014; Siegel et al., 2014]. Sometimes, the photosynthesis process brings to an intense reproduction and accumulation of algal cells and these algal blooms change the natural blue color of the sea, usually, toward a greenish color. More precisely, the color of seawater depends on the Inherent Optical Properties (IOPs), such as absorption and scattering, of water itself and

of some optically active constituents. These are: Chlorophyll [CHL] which is the main photosynthetic pigment, Colored Dissolved Organic Matter (CDOM), produced during the decaying of terrestrial vegetation or of marine phytoplankton and Non-Algal Particles (NAP), of which the Suspended Particulate Matter (SPM), can generally be an estimate. Such particulate is largely due to the river sediment discharges, resuspension of bottom particles and atmospheric input of dust [IOCCG, 2000]. Satellite data provide a synoptic view of the ocean with adequate spatial and temporal resolutions and represent a crucial tool for the knowledge of phytoplankton dynamics [Brewin et al., 2011]. Specific satellite sensors with good spatial and spectral resolutions, and especially with a high signal to noise ratio, were designed to observation of the color of the sea [McClain, 2009]. Among them, the most important are the Sea-viewing Wide Field of view Sensor (SeaWiFS), operating from 1997 to 2010, the MEdium Resolution Imaging Spectrometer (MERIS), in orbit from 2001 to 2012, and the last Moderate Resolution Imaging Spectroradiometer (MODIS) sensor installed on board the Aqua satellite, launched in 2002 and still in operation.

As regards [CHL] retrieval algorithms, the global OC3M, designed for MODIS data, is empirical and is derived from *in situ* measurements of [CHL] and the blue/green band ratios of remote sensing reflectance (Rrs) [O'Reilly et al., 2000]. The nominal uncertainty of OC3M algorithm in open seawaters is ± 35%, but this requirement is met only in the most oligotrophic zones of the world [Moore et al., 2009], while the [CHL] estimation errors may increase in optically complex waters, typically coastal seawaters. This is mostly due to the significant presence of other water optical constituents, which vary independently of [CHL], and to the inaccuracy of the atmospheric models applied. In particular for the latter issue, atmospheric corrections are crucial in turbid coastal seawaters and for the bluest bands of the spectrum [Antoine et al., 2008; Goyens et al., 2013].

Besides, the application of global algorithms may be not adequate in some marine regions such as the Baltic Sea, the Southwestern Atlantic Ocean and the Mediterranean Sea, due to their distinctive features [Volpe et al., 2007]. In particular, a significant overestimation of [CHL] is usually observed in the Mediterranean Sea, which has been attributed to its peculiar optical properties [Gitelson et al., 1996; Moulin et al., 2001; Claustre et al., 2002; D'Ortenzio et al., 2002]. Among others, Volpe et al. [2007] showed that the oligotrophic seawaters of the Mediterranean Sea are less blue (30%) and greener (15%) than those of the global ocean. This could be due to the presence of specific groups of phytoplankton [Santoleri et al., 2008] or to an unusually higher [CDOM] than that observed with respect the nearby Atlantic Ocean at the same latitude and in similar trophic conditions [Morel and Gentili, 2009]. Peculiar effects and dynamics of [CDOM] have also been found by Organelli et al. [2014] in the analysis of the data collected at the BOUSSOLE site (Ligurian Sea).

In order to address these peculiar optical properties of the Mediterranean Sea some regional algorithms have been developed, such as BRIC [Bricaud et al., 2002], DORMA [D'Ortenzio et al., 2002], MedOC4 [Volpe et al., 2007] for SeaWiFS and MedOC3 for MODIS [Santoleri et al., 2008]. MedOC3, in particular, is a regional empirical algorithm, similar to the global algorithm, but exclusively tuned for the Mediterranean Sea on a representative open seawater bio-optical data set.

Other types of algorithms, such as the semi-analytical ones, have been developed to derive the main optical constituents of seawater from multispectral Rrs observations by inverting the radiative transfer equations [Gordon and Morel, 1983]. In semi-analytical algorithms, the

inversion method requires a preliminary knowledge, obtained in an empirical way, of specific seawater optical features and then the derivation of [CHL] from IOPs [IOCCG, 2006].
The advantage of these methods is to retrieve simultaneously multiple ocean properties from a single Rrs spectrum [Tilstone et al., 2012]. In general, however, because of the local parameterization, the application of these algorithms outside the calibration areas requires a special care [Huang et al., 2013]. Various studies that use satellite remote sensing to predict [CHL] and primary production have been recently conducted in some sub-basins of the Western Mediterranean Sea (WMed), including the EU funded MOMAR Project (http://www.mo-mar.net) [Maselli et al., 2009; Lazzara et al., 2010a; Massi et al., 2011; Lapucci et al., 2012; Marchese et al., 2015]. In particular, Maselli et al. [2009] developed a semi-analytical algorithm (SAM_LT) for retrieving the three optical active constituents (CHL, CDOM, SPM) in the Ligurian and North Tyrrhenian Seas. SAM_LT is based on the Spectral Angle Mapping (SAM) technique [Sohn and Rebello, 2002; Chang et al., 2006] and, although initially designed for coastal seawaters, has been recently revisited and applied to open seawaters [Massi et al., 2011].
The primary objective of the current study is to assess the performance of the SAM_LT algorithm in comparison with those of the more renowned algorithms, OC3M and MedOC3. This assessment is carried out considering both the entire Western Mediterranean basin and only in the sea area where SAM_LT was developed and calibrated, using a significant number of [CHL] samples and quasi-simultaneous MODIS imagery taken in the period 2002-2011. The second objective is to evaluate the sensitivity of the three algorithms to the MODIS quality flags that are routinely provided with the standard ocean products. Such an evaluation is important to drive the operational selection of optimum algorithms depending on the relevant configuration of quality flags.

Study Area

The study area corresponds to the Western Mediterranean basin (Fig. 1).
In particular, it includes the sub-basins toward the West of Italian Peninsula, such as the Ligurian and Tyrrhenian Seas, the Gulf of Lion, the Provencal Basin, the Balearic Sea, the Algerian Sea and the Alboran Sea [Bricaud et al., 2002]. The westernmost Alboran Sea is linked to the North Atlantic Ocean through the Strait of Gibraltar, while the Strait of Sicily, to South-West of the study area, is the main connection with the Eastern Mediterranean basin.
In the coastal areas of WMed, the continental shelves (depth less of 200 m) are narrow with the exceptions of the Gulf of Lion, Balearic, Tunisia, Southwestern Sicily and Tuscan platforms. In the central part of WMed, the large Balearic abyssal plain reaches a depth of about 2800 m, but the deepest points of the basin is in the Southern Tyrrhenian Sea (3800 m). In the Strait of Sicily, the average depth is about 400 m. The surface flow of Atlantic water enters the basin and follows the continental coasts with a cyclonic (counterclockwise) movement. In general, during this travel, the seawater becomes denser and this involves a sinking and, at the end of the tour, intermediate and deep water currents return in the Atlantic Ocean through the Strait of Gibraltar [Millot, 1999]. In the WMed the currents system is very complex and in addition to coastal currents various gyres and eddies are formed with cyclonic and anticyclonic circulations [Robinson et al., 2001; El-Geziry and Bryden, 2010]. The WMed is considered a mainly oligotrophic basin and, in open seawaters, [CHL] rarely exceed the 2-3 mg m^{-3} [D'Ortenzio and Ribera d'Alcalà, 2009].

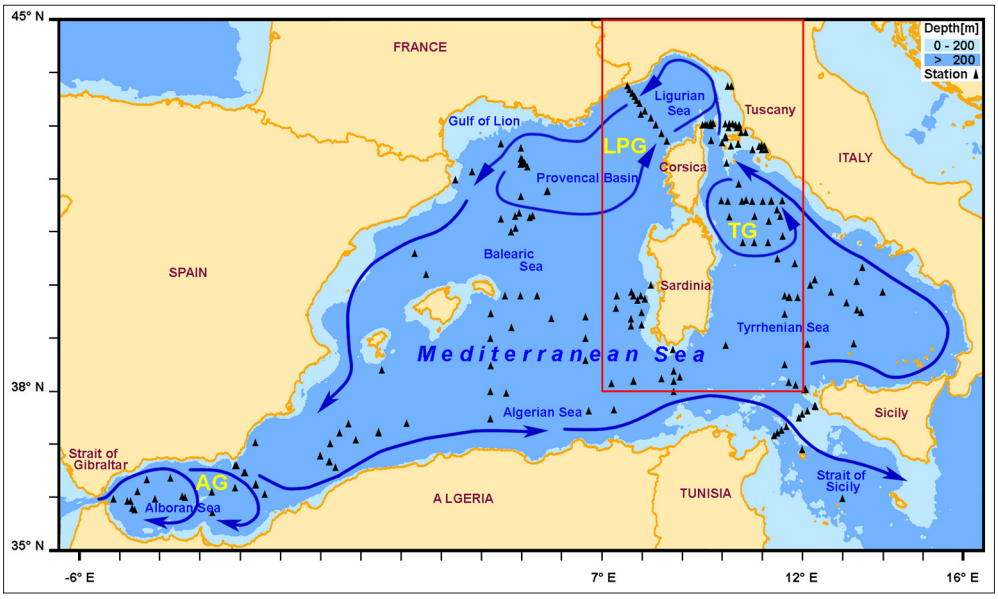

Figure 1 - Western Mediterranean Sea with the 240 measuring stations of [CHL] (Δ); The arrows indicate the surface circulation; LPG: Liguro-Provencal Gyre; TG: Tyrrhenian Gyre; AG: Alboran Gyre; the red box outlines the MOMAR area (7-12° E, 38-45° N).

Within some sub-basins, seasonally, cyclonic (Liguro-Provencal (LPG) and Tyrrhenian (TG)) and anticyclonic (Alboran (AG)) gyres are observed, in correspondence of which wide algal blooms develop shifting the typical oligotrophic status toward mesotrophic or eutrophic conditions [Morán and Estrada, 2001; Bosc et al., 2004; D'Ortenzio and Ribera d'Alcalà, 2009; Lazzara et al., 2010a; Marchese et al., 2015].The Liguro-Provencal and Alboran basins are among the most productive of the Mediterranean Sea [Siokou-Frangou et al., 2010]. Increased phytoplankton levels may also occur in coastal areas, especially near large river mouths, due to the nutrients available in the water. In addition to this, harmful algal blooms have been detected in many coastal areas, producing problems for human health and activities [Penna et al., 2007]; these blooms have been also observed in offshore mesoscale eddies, representing a 'seed bank' for further dispersion and spreading of the harmful species [Fani et al., 2014].

The red box in Figure 1 delimits a subarea which is currently considered to correspond to that of the MOMAR project, although the study area of respective Project was actually slightly smaller and centered on the Ligurian Sea. As previously mentioned, the current analyses were carried out considering both the entire WMed and only this subarea.

Materials and methods

In situ [CHL] measurements

In situ [CHL] measurements (240 samples) were collected in pelagic and neritic areas of WMed during several oceanographic campaigns carried out from 2002 to 2011 (Fig. 1, Tab. 1). Seawater sampling was carried out by means of 10 L Niskin bottles either alone (from

aboard R/V Blue Dream and Poseidon), or integrated in a rosette system (from aboard the CNR R/V Urania). In this study, we have used only seawater samples collected from the surface layer down to a depth of 3 m. This choice is justified by theoretical considerations on the optical properties of Mediterranean waters [D'Ortenzio and Prieur, 2012] and is a common practice for the calibration/validation of remote sensing [CHL] estimates in seawaters [Kahru et al., 2014].

Table 1 - Source and main features of *in situ* surface [CHL]: campaign, number of sampling points (N); average (MD), standard deviation (SD), maximum and minimum value (MAX and MIN) of [CHL]; year and season of sampling.

Campaign	N	MD [mg m^{-3}]	SD [mg m^{-3}]	MAX [mg m^{-3}]	MIN [mg m^{-3}]	Year season
MedGOOS5	1	0.129		0.129	0.129	2002 FALL
NORBAL4-5	29	1.583	1.330	6.004	0.103	2003 WINTER-SPRING
MedGOOS7	14	0.555	0.314	1.085	0.229	2004 WINTER
MedGOOS8	27	0.108	0.078	0.327	0.034	2004 SPRING
MedGOOS9	25	0.123	0.090	0.398	0.066	2004 FALL
MedGOOS10	14	0.251	0.286	0.998	0.039	2005 SPRING
MedGOOS11	5	0.212	0.117	0.408	0.099	2005 FALL-WINTER
MedGOOS12	2	0.158	0.089	0.221	0.095	2006 SPRING
MedGOOS13	28	0.197	0.216	1.085	0.042	2006 FALL
MedBio06	16	0.115	0.062	0.240	0.062	2006 FALL
MedOcc07	36	0.139	0.068	0.364	0.069	2007 FALL
MedCO08	14	0.294	0.209	0.712	0.118	2008 FALL
BO2010SIC	2	0.217	0.042	0.247	0.187	2010 WINTER
MOMAR-1	2	2.306	0.556	2.699	0.556	2011 WINTER
MOMAR-2	12	0.123	0.035	0.205	0.035	2011 SPRING
MOMAR-3	3	0.062	0.013	0.070	0.013	2011 SUMMER
MOMAR-4	10	0.188	0.168	0.581	0.168	2011 FALL

For phytoplankton chlorophyll analyses, four liters of seawater were filtered on glass-fiber filter Whatman GF/F (Ø 47 mm). After filtration, filters were immediately frozen until extraction in acetone 90% at 4°C for one day. Chlorophyll-a was analyzed by spectrophotometry using monochromatic equation [Lazzara et al., 2010b]. In addition to this, in most recent samples also the high-performance liquid chromatography HPLC (SHIMAZDU Class VP) using a reverse-phase RP-C8 column was performed. The procedure was able to separate Chlorophyll-a from divinyl-Chlorophyll-a [Vidussi et al., 1996; Barlow et al., 1997]. The sum of Chlorophyll-a and divinyl-Chlorophyll-a concentrations, named [Tchl-a], was compared to [CHL] obtained from the monochromatic method. The results are summarized in the following regression:

[Tchl-a] = 0.870 [CHL] , with N = 27 and r^2 = 0.998 (highly significant correlation, P<0.01). This Equation was applied to correct the [CHL] observations of all sea samples.

MODIS data

MODIS is an instrument on board of Aqua, an orbiting polar satellite launched by NASA. It has a viewing swath width of 2330 km and views the entire surface of the Earth about every two days. MODIS has 36 spectral bands covering the spectral range from visible to infrared bands (412-14200 nm), and the sensor spatial resolution at nadir varies from 250 m and 1000 m, depending on the bands. Usually, in the Ocean Color (OC) analysis, the bands in the range 412-678 nm are used, for most of which the signal to noise ratio (SNR) is optimal [Xiong et al., 2004]. Instead, the thermal and middle infrared bands provide information on the Sea Surface Temperature (SST) that can improve understanding of physical environment affecting the distribution and dynamics of phytoplankton [Bricaud et al., 2002]. MODIS data are collected and processed at different levels by Ocean Biology Processing Group (OBPG) at NASA's Goddard Space Flight Center, and distributed through the NASA OceanColor Web (http://oceancolor.gsfc. nasa.gov). NASA has also developed a software package for satellite data processing, the SeaWiFS Data Analysis System (http://seadas.gsfc.nasa.gov). The SeaDAS version used in this study is the 7.0.2. Data processing details can be found at http://oceancolor.gsfc.nasa.gov/DOCS/MODISA_processing.html.

The geophysical products are provided at the second level (L2) of processing of data and they are calibrated and corrected atmospherically and geometrically. The procedures applied for the atmospheric correction and the application of bio-optical algorithms are continuously validated by high quality *in situ* measurements. As for other NASA satellite missions, periodically, OBPG applies a partial, or total, reprocessing of distributed data when advances in algorithms or sensor calibration knowledge can significantly improve product quality or utility. The reprocessing version, applied to the MODIS data set used in this analysis, is the 2013.1. All L2 products include numerous metadata to characterize the quality of each retrieved pixel values, such the date, time, and coordinates of data collection. Additionally, numerous flags are provided to indicate if any algorithm failures or warning occurred for each pixel of the scene.

In this study, for each MODIS scene analyzed, the following L2 products were selected: Rrs in ten bands (412, 443, 469, 488, 531, 547, 555, 645, 667, 678 [nm]), [CHL] derived from the OC3M algorithm and the l2_flags band.

The special l2_flags band contains quality flag information. These flags allow an assessment of some tests and conditions that may affect the quality of data or of the algorithms associated to various products (Tab. 2). Basically, the flag data set always have a 4-byte integer, showing 32 possible bilevel flags, associated to each image pixel indicating various conditions on the standard products. If the bit value is flagged (i.e. equal to one), the specific test or condition occurs; consequently, the pixel can be excluded from the analysis or, in case it is used, a particular care is needed. A description of most of the flags can be found in Robinson et al. [2003] although later, especially with the 2009 reprocessing (http://oceancolor.gsfc.nasa.gov/REPROCESSING/R2009/flags) some changes have been applied. A short description of the flags most relevant for the current study follows. Some flags are set based on threshold values:

a) HILT is flagged if any of the bands or detectors reach the physical saturation. This

condition is determined if the raw digital count of the pixel examined, at level 1B, is equal to or exceeds 65500;

b) HIGLINT and MODGLINT are flagged if for that pixel the glint reflectance exceeds respectively 0.005 and 0.0001;

c) HISATZEN is flagged if 60 degree satellite zenith threshold is reached.

Sometimes some flags are present in large numbers on a scene and therefore they can hardly be excluded from the data analysis.

Table 2 - Main features of l2_flags: bit position, name ad description of the algorithms associated to the flags.

Bit	Flag name	Description
1	ATMFAIL	Atmospheric correction failure
2	LAND	Land
3	PRODWARN	One (or more) product algorithms generated a warning
4	HILT	High (or saturating) TOA radiance
5	HIGLINT	High glint determined
6	HISATZEN	Large satellite zenith angle
7	COASTZ	Shallow water (<30 m)
8	unused	
9	STRAYLIGHT	Stray light determined
10	CLDICE	Cloud or ice determined
11	COCCOLITH	Coccolithofores detected
12	TURBIDW	Turbid water detected
13	HISOLZEN	High solar zenith angle
14	unused	
15	LOWLW	Low Lw at 555 nm (possible cloud shadow)
16	CHLFAIL	Chlorophyll algorithm failure
17	NAVWARN	Navigation suspect
18	ABSAER	Absorbing Aerosol determined
19	unused	
20	MAXAERITER	Maximum iterations reached for NIR iteration
21	MODGLINT	Moderate glint determined
22	CHLWARN	Chlorophyll out-of-bounds (<0.01 or >100mg m^{-3})
23	ATMWARN	Atmospheric correction warning: Epsilon out-of-bounds
24	unused	
25	SEAICE	Sea ice determined
26	NAVFAIL	Navigation failure
27	FILTER	Insufficient data for smoothing filter
28	SSTWARN	SST suspect
29	SSTFAIL	SST algorithm failure
30	HIPOL	High degree of polarization determined
31	PRODFAIL	One (or more) product algorithms produced a failure
32	unused	

A typical example is STRAYLIGHT, the flag that indicates the influence of brightness of adjacent pixels on pixel reflectance value. Usually, this phenomenon occurs in proximity of coastlines and on the edge of clouds. Since the scenes, as often occurs, have a partial cloud cover, the number of flagged pixels will be high. OBPG suggests that the effect of contamination can be eliminated with a 5x3-pixel masking around these high-radiance pixels (http://oceancolor.gsfc.nasa.gov/REPROCESSING/Aqua/R1/modisa_repro1_stlight .html). The ABSAER flag indicates the presence of an absorbing aerosol. However, this flag is not generally taken into consideration because the detection algorithm is still unreliable (http://oceancolor.gsfc.nasa.gov/forum/oceancolor/topic_show.pl?tid=4668).
The PRODFAIL flag, indicating at least one failure in the construction of all L2 products, is also sometimes ignored in the analysis of the sea color because the product failure can be due to Sea Surface Temperature disturbance (also indicated by SSTWARN and SSTFAIL) and can therefore be related to phenomena other than those investigated.
Many flags have been defined for different types of sensor (SeaWiFS, MERIS, MODIS) others were defined only for a specific sensor. For example, HIPOL, the flag that indicates when a high degree of polarization of the light reflected from the sea surface occurs, is defined only for the MODIS sensor.
Finally, some flags are used to mask the standard products at each data processing level. For example, if the flags LAND and CLDICE are raised then a mask pixel is applied to MODIS L2 data.
Similarly, the following flagged pixels are masked to MODIS L3 data: ATMFAIL, LAND, HIGLING, HILT, HISATZEN, STRAYLIGHT, CLDICE, COCCOLITH, HISOLZEN, LOWLW, CHLFAIL, NAVWARN, MAXAERITER, CHLWARN, ATMWARN, NAVFAIL and FILTER.

The CHL algorithms considered

OC3M and MedOC3

The OC3M algorithm is a fourth degree polynomial regression between log-transformed [CHL] and log-transformed Maximum Band Ratio (MBR) of Rrs [O'Reilly et al., 2000]:

$$[CHL] = 10^{C_0 + C_1 \cdot R + C_2 \cdot R^2 + C_3 \cdot R^3 + C_4 \cdot R^4} \qquad [1]$$

where:

$$R = log_{10} max\left(\frac{Rrs_{443}}{Rrs_{547}}, \frac{Rrs_{488}}{Rrs_{547}}\right)$$

The blue/green ratio has the advantage of normalizing internal and external conditions (scattering coefficient variability, geometry, incident radiance at the surface). The MBR has the additional advantage of maintaining the highest possible satellite sensor signal-to-noise ratio over a 3-orders-of-magnitude in the [CHL] [O'Reilly et al., 1998]. The coefficients of Equation [1] were obtained using *in situ* data from the NASA bio-Optical Marine Algorithm Data set (NOMAD) version 2 (http://oceancolor.gsfc.nasa.gov/REPROCESSING/R2009/ocv6) [Werdell and Bailey, 2005]. The NOMAD data set includes coincident observations of spectral water-leaving radiances and [CHL], along with relevant metadata.
The OC3M global algorithm were developed using an wide *in situ* data set consisting of

both open and coastal seawaters with the approximate range of 0.012<[CHL]<72.12 mg m^{-3} [Werdell and Bailey, 2005].
The MedOC3 algorithm, like OC3M, is based on a fourth power polynomial regression between log-transformed [CHL] and log-transformed MBR (Eq. [1]). This algorithm was calibrated on a representative open seawaters bio-optical data set collected in the Mediterranean area and was developed using data set within the range of 0.003<[CHL]<7.06 mg m^{-3} [Volpe et al., 2007; Santoleri et al., 2008].
Table 3 reports the coefficients used in the OC3M and MedOC3 algorithms.

Table 3 - Coefficients of Equation [1] for OC3M and MedOC3 algorithms.

	C_0	C_1	C_2	C_3	C_4
OC3M	0.2424	-2.7423	1.8017	0.0015	-1.2280
MedOC3	0.3800	-3.6880	1.0360	1.6160	-1.3280

SAM_LT
The CHL semi-analytical algorithm SAM_LT, initially proposed for the coastal areas of Tuscany Region by Maselli et al. [2009], has been adapted by Massi et al. [2011] to improve its performance in open seawaters. The original method compares the Rrs directly measured by MODIS in each of the 240 pixels containing the sampling station (Rrs_{meas}) with the simulated remote sensing reflectance (Rrs_{sim}) obtained through the following equation:

$$Rrs_{sim.} = 0.051 \frac{b_{bw} + [CHL] \cdot b^*_{b_{PH}} + [SPM] \cdot b^*_{b_{NAP}}}{a_w + [CHL] \cdot a^*_{PH} + [SPM] \cdot a^*_{NAP} + [CDOM] \cdot a^*_{CDOM}} \quad [2]$$

where [CHL], [SPM] and [CDOM] are the concentrations of Chlorophyll-a, NAP and CDOM, respectively; a_w is the absorption coefficient of pure seawater, a^*_{PH}, a^*_{NAP} and a^*_{CDOM} are the specific absorption coefficients of phytoplankton, NAP and CDOM; b_{bw} is the backscattering coefficient of pure seawater, $b^*_{b_{PH}}$, $b^*_{b_{NAP}}$ are the specific backscattering coefficients of phytoplankton and NAP.
The comparative analysis identifies a minimum of an error function that is based on the cosine of the angle between the standardized vectors of measured and simulated reflectances, $\cos\theta_{MS}$.
$\cos\theta_{MS}$ is equivalent to the correlation coefficient and measures the similarity in shape between the two reflectance vectors without detecting spectral amplitude differences [Sohn and Rebello, 2002; Chang et al., 2006]. In this way, the algorithm is insensitive to amplitude variations of the measured reflectances, which may be due to the presence of seawater constituents with variable amplitude of the absorption properties but with similar spectral features and/or to inaccurate atmospheric correction of the satellite data [Maselli et al., 2009].
Since all specific absorption and backscattering coefficients used in Equation [2] are obtained from a bio-optical survey of the Ligurian and North Tyrrhenian Seas, the algorithm has intrinsically a local validity.
In the modified version of Massi et al. [2011] the algorithm, then called SAM_LT, has been tuned in open seawaters based on the relationships [CHL]/[NAP] and [CHL]/[CDOM], both obtained from a bio-optical survey of local open seawaters.

In this case, the algorithm is first applied to characterize the proximity of each estimation point (pixel) to open seawaters. Next, the same algorithm is used to estimate the concentrations of CHL and related optically active constituents in these seawaters, while the original method is applied to predict the concentration of all constituents in coastal seawaters.
The final prediction is obtained as a weighted average of [CHL] estimates in open and coastal seawaters (see Massi et al. [2011], for details). More specifically, these two types of waters, in the bio-optical classification of Morel and Prieur [1977], correspond to Case 1 (C1W) and Case 2 (C2W) waters, respectively. Therefore, the [CHL] estimation with SAM_LT algorithm is obtained through the following equation:

$$[CHL]_{SAM\_LT} = cos\theta_{MS} \cdot [CHL]_{SAM(C1W)} + (1 - cos\theta_{MS}) \cdot [CHL]_{SAM(C2W)} \quad [3]$$

Where $[CHL]_{SAM(C1W)}$ and $[CHL]_{SAM(C2W)}$ are the $[CHL]_{SAM\_LT}$ estimates obtained by the algorithm versions for open and coastal seawaters, respectively.
Since the algorithm of Massi et al. [2011] for open seawaters is very sensitive to the adopted relationship between the concentration of CHL and those of the other optically active constituentes, a simulation trial was also perfomed replacing the original relationship [CHL]/[CDOM] with that reported in Equation [3] of Morel and Gentili [2009]. This variant of SAM_LT algorithm is hereinafter indicated with the name of SAM_LT_{mod}.

Data processing

According to the dates and the coordinates of the CHL sampling points all L2 MODIS scenes from the NASA archive containing the *in situ* locations were downloaded. Then, the values of the standard products, including the Rrs of all available bands, the OC3M [CHL] and all flags, were extracted from each MODIS scene for each pixel sampled, using scripts built with the Graph Processing Tool of the SeaDAS package. At the latitudes of the study area, a satellite overpass is usually available for each day, which was currently considered. Sometimes, however, the scenes of each day can be two, i.e. an overpass in the morning and another in the afternoon. In these cases, the measured [CHL] was associated to both remotely sensed values. The extracted values of Rrs in the suitable MODIS bands were used to apply the MedOC3 and SAM_LT algorithms for [CHL] retrieval. All [CHL] estimates were then compared to the [CHL] measurements both for the entire Western Mediterranean basin and only for the MOMAR area. The results of the comparisons were summarized by means of common accuracy statistics, i.e. the correlations coefficient (r), the root mean square error (RMSE) and the mean bias error (MBE).
Finally, the impact of main MODIS quality flags on [CHL] estimation accuracy was assessed by selecting samples with flagged pixels. In particular, the RMSEs of the three algorithms were again computed for the flags that showed a significant number of occurrences (more than 10%).

Results

Performances of the three algorithms

Considering the entire Western Mediterranean basin, 240 samples were found corresponding to MODIS imagery for which the estimation of OC3M [CHL] was feasible. The visual analysis

of these spectra indicated that most of them have typical open seawater features, i.e. they are optically dominated by [CHL]. This was confirmed by the corresponding SAM_LT correlations with open seawaters, which had a mean value of about 0.9. Figure 2 shows the results of the accuracy assessment of the three algorithms for these 240 samples. OC3M provides the best results, while SAM_LT strongly underestimates [CHL]. As regards the modified version of the algorithm (SAM_LT_{mod}), it substantially reduces the previously observed [CHL] underestimation, producing errors that are similar to those of the other algorithms.
Table 4 reports the same accuracy statistics for the MOMAR area, where 115 samples were found. In this case, the SAM_LT algorithm provides the best accuracy, which is further improved by SAM_LT_{mod}.

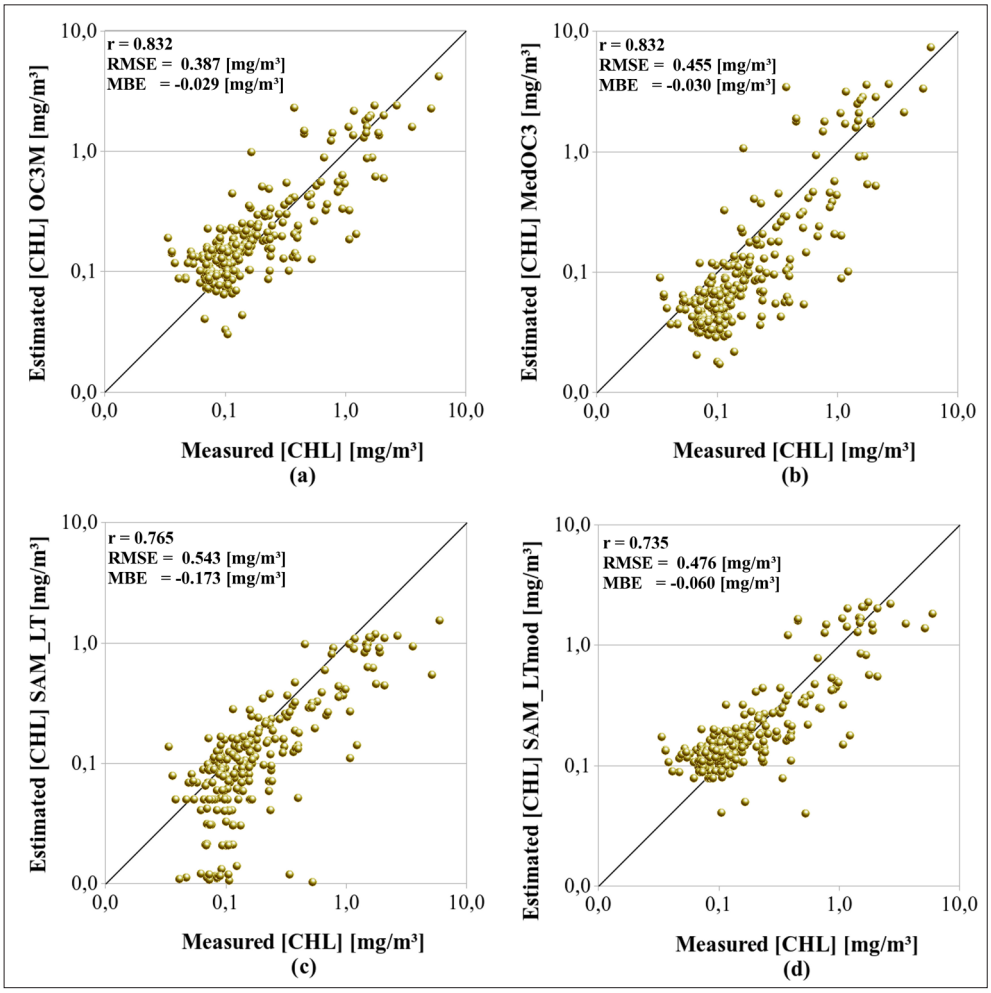

Figure 2 - [CHL] measured versus estimated by the algorithms considered: a=OC3M, b=MedOC3, c=SAM_LT, d=SAM_LT_{mod} (N=240, r with highly significant correlation, P < 0.01).

Effects of flags

All together, the flagged pixels covered a large majority of the 240 WMed samples examined, as only 35 of these were fully unflagged. Table 5 reports the accuracy statistics of the [CHL] algorithms for these unflagged pixels. As expected, the accuracy of all algorithms is significantly improved, with a notable reduction of the error levels.

Figure 3 shows the percentages of flagged pixels within the same 240 samples. Only seven flags (HISATZEN, STRAYLIGHT, ABSAER, MODGLINT, SSTWARN, HIPOL, PRODFAIL) that were present in more than 10% of the samples have been selected for the error analysis of the three algorithms.

Figure 4 shows the mean error levels obtained by the three algorithms when considering only flagged pixels.

Table 4 - Accuracy statistics of [CHL] estimation algorithms obtained for the MOMAR area (N = 115, r with highly significant correlation, P < 0.01).

	OC3M	MedOC3	SAM_LT	SAM_LT_{mod}
r	0.758	0.752	0.885	0.897
RMSE	0.221	0.326	0.201	0.137
MBE	0.031	-0.020	-0.064	0.004

Table 5 - Accuracy statistics of [CHL] estimation algorithms obtained for the Western Mediterranean Sea with fully unflagged pixels (N=35, r with highly significant correlation, P < 0.01).

	OC3M	MedOC3	SAM_LT	SAM_LT_{mod}
r	0.986	0.996	0.952	0.988
RMSE	0.148	0.119	0.197	0.155
MBE	-0.071	-0.130	-0.166	-0.091

While the MedOC3 errors are significantly higher than those obtained with the other algorithms for the STRAYLIGHT and SSTWARN flags, the mean errors of OC3M and SAM_LT are significantly different for STRAYLIGHT, ABSAER and PRODFAIL. In the first case, SAM_LT provides the best results, while the opposite is true for the other two cases.

Discussion and Conclusions

Various regional (empirical and semi-analytical) algorithms have been developed to attempt to correct the [CHL] errors produced by standard algorithms (e.g. OC3M) that, in the Mediterranean Sea, generally overestimate low [CHL] and, conversely, underestimate high [CHL] [Navarro et al., 2014]. In this study, the accuracy of three algorithms (OC3M, MedOC3 and SAM_LT) based on MODIS imagery was tested for the WMed. The analysis was made using a series of [CHL] measurements collected during various oceanographic cruises or activities in the 2002-2011 decade. The results are mostly in accordance with those of previous investigations. This study indicates a slight tendency to [CHL] underestimation of the more common algorithms (OC3M and MedOC3), similar to that found by other authors [Volpe et al., 2012].

These results, however, are apparently in contradiction with those found by other authors on a regional scale. For example, Santini et al. [2007] found a clear [CHL] overestimation

of the same algorithms and particularly of OC3M. This finding was at least partly due to the prevalent consideration of coastal seawaters, where other optically active seawater constituents (SPM and CDOM) alter the green/blue ratios which are the basis of the global algorithm. Conversely, the current prevalence of open seawaters is the most likely cause of the strong [CHL] underestimation obtained by SAM_LT, which is particularly evident in the most productive seawaters of the Gulf of Lion, mainly characterized by the NORBAL 2003 campaign. The open seawaters version of this algorithm, which is mostly active in the current case, was, in fact, calibrated in WMed oligotrophic areas where [CHL] was below 1 mg m^{-3} [Massi et al., 2011]. Consequently, all relationships linking the [CHL] to that of the other optically active constituents are not tuned for high [CHL] levels, and all optical equations used to retrieve absorption and backscattering coefficients may also be suboptimal for these conditions. This explains the above mentioned strong [CHL] underestimation found for the most productive open seawater samples. It can therefore be hypothesized that one of the main weaknesses of the SAM_LT algorithm for open seawaters is related to the use of a linear relationship between [CHL] and [CDOM], which cannot be correctly extended to the most productive areas of WMed. This is confirmed by the simulation performed using the modified algorithm SAM_LT_{mod}, which uses the power dependence of [CDOM] on [CHL] proposed by Morel and Gentili [2009]. This trial leads to a decisive improvement of the [CHL] estimates, reducing the underestimation for both very high and low [CHL] levels. The previous considerations can also explain the different results found when considering only the MOMAR area. The open seawater samples taken in this area, in fact, show [CHL] values lower than 1 mg m^{-3}. In these cases, the conventional algorithms provide errors only slightly lower than those obtained for the entire study area, while the [CHL] estimates of SAM_LT are highly improved (Tab. 4). Thus, the last algorithm produces the best accuracy, although still maintains a certain tendency to underestimation. Again, this tendency is completely removed by the use of the modified version of the algorithm (SAM_LT_{mod}).

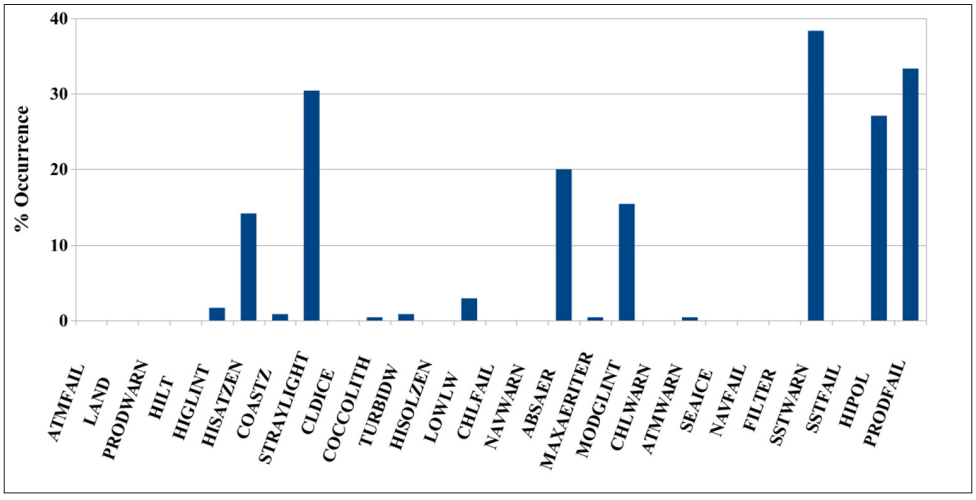

Figure 3 - Percent occurrence of flagged pixels within the 240 Western Mediterranean Sea samples.

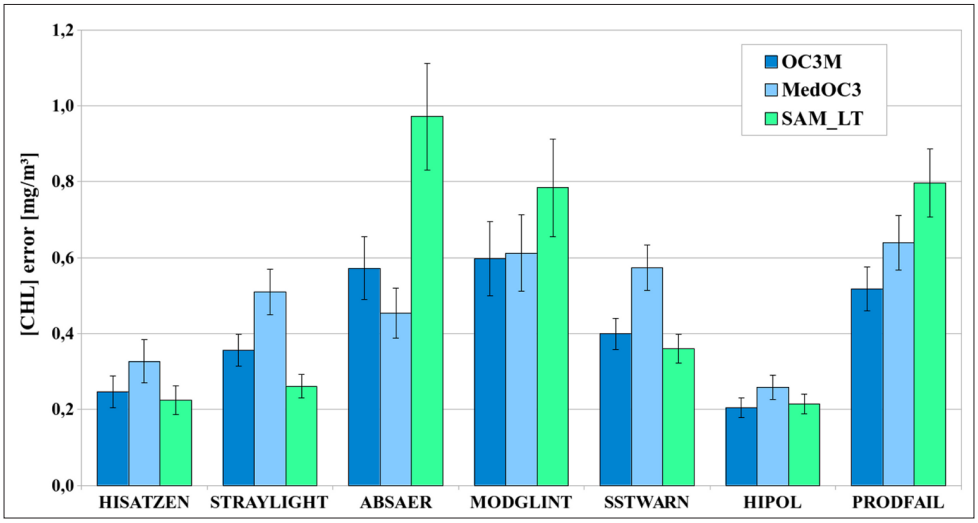

Figure 4 - Mean error levels and confidence intervals obtained by the three basic algorithms for flagged pixels.

These results indicate that the application of the SAM_LT algorithm in the WMed would require a recalibration based on a bio-optical survey and aimed at better defining the specific inherent optical properties (absorption and backscattering) of the optically active seawater constituents for the study area. This operation is actually straightforward, since the flexibility of this semi-analytical algorithm allows its simple upgrading, using the most appropriate relationships that were defined in Massi et al. [2011]. From an operational viewpoint, such an upgrading would be extremely rewarding, as it would allow the contemporaneous estimation of the main optically active constituents in the entire WMed.

The second part of the study concerned the evaluation of MODIS quality flags for [CHL] retrieval. The importance of this assessment can be fully comprehended considering that common data analysis procedures often include a filtering of pixels based on the quality flags, especially in data set validation or vicarious calibration programs. In fact, before analyzing the data, a selection of relevant flags is usually made and the flagged pixels are removed from the analysis [Bailey et al., 2008; Volpe et al., 2012; Kahru et al., 2014; Zibordi et al., 2015]. Of course, this filtering can involve a considerable reduction of the number of samples with the exclusion of information that is not necessarily wrong. This is confirmed by the results of the current analysis, which indicate the relative rarity of fully unflagged MODIS pixels in the study area. Such pixels, in fact, represent only a small minority (less than 15%) of those for which OC3M [CHL] is available. Using only these pixels would therefore lead to improve the obtainable [CHL] estimates (Tab. 5), but at the expense of their number, and therefore of a reduced statistical significance.

In general, the analysis of the most relevant flags (Fig. 4) provides indications that can be interpreted on the basis of bio-optical considerations. The best performance of the SAM_LT algorithm when STRAYLIGHT is flagged is likely due to the contemporaneous consideration of all spectral information provided by 10 MODIS bands, which attenuates the effect of incorrect blue/green reflectance ratios. The presence of stray light, in fact, alters

the blue/green ratio leading to significant [CHL] overestimation [Terauchi et al., 2014]. On the contrary, the consideration of all spectral bands reduces the efficiency of SAM_LT when ABSAER is flagged, since the absorbing aerosol shows variable spectral properties that could affect all regions of the reflectance spectrum. A similar interpretation can be valid for the PRODFAIL flag, which may be due also to disturbed atmospheric conditions. In conclusion, the current study has fulfilled its research objectives, providing useful guidelines for the operational utilization of the three [CHL] algorithms in the Western Mediterranean basin. Additionally, some indications are yielded on the possible modifications of the regional SAM_LT algorithm, which could improve its efficiency in the whole WMed area. As regards the quality flags, it should be reminded that they are mainly usable with L2 data, which are provided with the highest spatial resolution for each single MODIS scene. Conversely, in MODIS L3 data, which are usually aggregated at lower spatial and temporal resolutions, most of the flags are automatically masked. The current results therefore provide guidelines for using MODIS L2 data sets in the WMed, and their relevance is not restricted to this data, since similar flags are associated to data from other sensors (SeaWiFS, MERIS).

Acknowledgements

Most of the sea [CHL] samples used in the current study were collected during cruises and campaigns funded by EU, CNR and ASI (Tab. 1); these contributions are gratefully acknowledged. Dr. C. Santini is thanked for her helpful comments on the first draft of the manuscript.

Thanks are also due to ISMAR-CNR and IAMC-CNR for giving hospitality aboard the R/V 'Urania', to its captains and crews for their assistance and continuous support, as well as to those of the R/V "Blue Dream" and R/V "Poseidon".

References

Alvain S., Duforêt-Gaurier L., Loisel H. (2011) - *Observation of Ocean Colour Beyond Chlorophyll-a: From Particulate Organic Carbon Content and Size Distribution to Phytoplankton Functional Groups*. In: Handbook of Satellite Remote Sensing Image Interpretation: Applications for Marine Living Resources Conservation and Management, Morales J., Stuart V., Platt T., Sathyendranath S. (Eds.), EU PRESPO and IOCCG, Dartmouth, Canada, pp. 65-77.

Antoine D., D'Ortenzio F., Hooker S.B., Be´cu G., Gentili B., Tailliez D., Scott A.J. (2008) - *Assessment of uncertainty in the ocean reflectance determined by three satellite ocean color sensors (MERIS, SeaWiFS and MODIS-A) at an offshore site in the Mediterranean Sea (BOUSSOLE project)*. Journal of Geophysical Research: Oceans, 113 (C07013). doi: http://dx.doi.org/10.1029/2007JC004472.

Bailey S.W., Hooker S.B., Antoine D., Franz B.A., Werdell P.J. (2008) - *Sources and assumptions for the vicarious calibration of ocean color satellite observations*. Applied Optics, 47 (12): 2035-2045. doi: http://dx.doi.org/10.1364/AO.47.002035.

Barlow R.G., Cummings D.G., Gibb S.W. (1997) - *Improved resolution of mono- and divinyl chlorophylls a and b and zeaxanthin and lutein in phytoplankton extracts using reverse phase C-8 HPLC*. Marine Ecology Progress Series, 161: 303-307. doi: http://dx.doi.org/10.3354/meps161303.

Bosc E., Bricaud A., Antoine D. (2004) - *Seasonal and interannual variability in algal biomass and primary production in the Mediterranean Sea, as derived from four years of SeaWiFS observations*. Global Biogeochemical Cycles, 18 (GB1005). doi: http://dx.doi.org/10.1029/2003GB002034.

Brewin R.J.W., Hardman-Mountford N.J., Lavender S.J., Raitsos D.E., Hirata T., Uitz J., Devred E., Bricaud A., Ciotti A., Gentili B. (2011) - *An intercomparison of bio-optical techniques for detecting phytoplankton size class from satellite remote sensing*. Remote Sensing of Environment, 115 (2): 325-339. doi: http://dx.doi.org/10.1016/ j.rse.2010.09.004.

Bricaud A., Bosc E., Antoine D. (2002) - *Algal biomass and sea surface temperature in the Mediterranean Basin: Intercomparison of data from various satellite sensors, and implications for primary production estimates*. Remote Sensing of Environment, 81: 163-178. doi: http://dx.doi.org/10.1016/S0034-4257(01)00335-2.

Chang G.C., Barnard A.H., McLean S., Egli P.J., Moore C., Zanevel J.R.V., Dickey T.D., Hanson A. (2006) - *In situ optical variability and relationships in the Santa Barbara Channel: implications for remote sensing*. Applied Optics, 45 (15): 3593-3604. doi: http://dx.doi.org/10.1364/AO.45.003593.

Claustre H., Morel A., Hooker S.B., Babin M., Antoine D., Oubelkheir K. (2002) - *Is Desert Dust Making Oligotrophic Waters Greener?* Geophysical Research Letters, 29 (10): 1071-1074. doi: http://dx.doi.org/10.1029/2001GL014056.

D'Ortenzio F., Marullo S., Ragni M., Ribera d'Alcala M., Santoleri R. (2002) - *Validation of Empirical SeaWiFS Algorithms for Chlorophyll-Alpha Retrieval in the Mediterranean Sea: Case Study for Oligotrophic Seas*. Remote Sensing of Environment, 82 (1): 79-94. doi: http://dx.doi.org/10.1016/S0034-4257(02)00026-3.

D'Ortenzio F., Ribera d'Alcalà M. (2009) - *On the trophic regimes of the Mediterranean Sea: a satellite analysis*. Biogeosciences, 6: 139-148. doi: http://dx.doi.org/10.5194/bg-6-139-2009.

D'Ortenzio F., Prieur L. (2012) - *The upper mixed layer*. In: Life in the Mediterranean Sea: A look at habitat changes, Noga Stambler (Ed.), Nova Science Publisher, pp. 127-156.

El-Geziry T.M., Bryden I.G. (2010) - *The circulation pattern in the Mediterranean Sea: issues for modeller consideration*. Journal of Operational Oceanography, 3 (2): 39-46. doi: http://dx.doi.org/10.1080/1755876X.2010.11020116.

Fani F., Nuccio C., Lazzara L., Massi L., Battocchi C., Penna A. (2014) - *Fibrocapsa japonica (Raphidophyceae) occurrence and ecological features within the phytoplankton assemblage of a cyclonic eddy, offshore the Eastern Alboran Sea*. Mediterranean Marine Science, 15 (2): 250-262. doi: http://dx.doi.org/10.12681/ mms.398.

Gitelson A., Karnieli A., Goldman N., Yacobi Y.Z., Mayo M. (1996) - *Chlorophyll estimation in the Southeastern Mediterranean using CZCS images: adaptation of an algorithm and its validation*. Journal of Marine Systems, 9 (3-4): 283-290. doi: http://dx.doi.org/10.1016/S0924-7963(95)00047-X.

Gordon H., Morel A. (1983) - *Remote Assessment of Ocean Color for Interpretation of Satellite Visible Imagery: A Review*. In: Lecture Notes on Coastal and Estuarine Studies, 4, Springer Verlag, New York, pp. 114. doi: http://dx.doi.org/10.1029/ln004.

Goyens C., Jamet C., Schroeder T. (2013) - *Evaluation of four atmospheric correction algorithms for MODIS-AQUA images over contrasted coastal waters*. Remote Sensing of Environment, 131: 63-75. doi: http://dx.doi.org/10.1016/j.rse.2012.12.006.

Gregg W.W., Rousseaux C.S. (2014) - *Decadal trends in global pelagic ocean chlorophyll: A new assessment integrating multiple satellites, in situ data, and models.* Journal of Geophysical Research: Oceans, 119: 5921-5933. doi: http://dx.doi.org/10.1002/2014JC010158.

Huang J., Chen L., Chen X., Song Q. (2013) - *Validation of semi-analytical inversion models for inherent optical properties from ocean color in coastal Yellow Sea and East China Sea.* Journal of Oceanography, 69 (6): 713-725. doi: http://dx.doi.org/10.1007/s10872-013-0202-8.

IOCCG (2000) - *Remote sensing of ocean colour in coastal and other optically complex, waters*. In: Reports of the International Ocean-Colour Coordinating Group, Sathyendranath S. (Ed.), 3, Dartmouth, Canada.

IOCCG (2006) - *Remote Sensing of Inherent Optical Properties: Fundamentals, Tests of Algorithms, and Applications*. In: Reports of the International Ocean-Colour Coordinating Group, Lee Z.P. (Ed.), 5, Dartmouth, Canada.

Kahru M., Kudela R.M., Anderson C.R., Manzano-Sarabia M., Mitchell B.G. (2014) - *Evaluation of Satellite Retrievals of Ocean Chlorophyll-a in the California Current*. Remote Sensing, 6: 8524-8540. doi: http://dx.doi.org/10.3390/rs6098524.

Lapucci C., Rella M.A., Brandini C., Ganzin N., Gozzini B., Maselli F., Massi L., Nuccio C., Ortolani A., Trees C. (2012) - *Evaluation of empirical and semi-analytical chlorophyll algorithms in the Ligurian and North Tyrrhenian Seas*. Journal of Applied Remote Sensing, 6 (1). doi: http://dx.doi.org/10.1117/1.JRS.6.063565.

Lazzara L., Marchese C., Massi L., Nuccio C., Maselli F., Santini C., Pieri M., Sorani V. (2010a) - *Sub-regional patterns of primary production annual cycle in the Ligurian and North Tyrrhenian seas, from satellite data*. Italian Journal of Remote Sensing, 42 (2): 87-102. doi: http://dx.doi.org/10.5721/ItJRS20104227.

Lazzara L., Bianchi F., Massi L., Ribera D'Alcalà M. (2010b) - *Pigmenti clorofilliani per la stima della biomassa fotototrofa.* In: Metodologie di campionamento e di studio del plancton marino, Socal G., Buttino I., Cabrini M., Mangoni O., Penna A., Totti C. (Eds.), ISPRA-SIBM, Roma, Manuali e Linee guida 56/2010, pp. 365-378.

Marchese C., Lazzara L., Pieri M., Massi L., Nuccio C., Santini C., Maselli F. (2015) - *Analysis of chlorophyll-a and primary production dynamics in north Tyrrhenian and Ligurian coastal-neritic and ocean waters*. Journal of Coastal Research, 31 (3): 690-701, Coconut Creek (Florida). doi: http://dx.doi.org/10.2112/JCOASTRES-D-13-00210.1.

Maselli F., Massi L., Pieri M., Santini C. (2009) - *Spectral Angle Minimization for the Retrieval of Optically Active Seawater Constituents from MODIS Data*. Photogrammetric Engineering & Remote Sensing, 75 (5): 595-605. doi: http://dx.doi.org/10.14358/PERS.75.5.595.

Massi L., Santini C., Pieri M., Nuccio C., Maselli F. (2011) - *Use of MODIS imagery for the optical characterization of Western Mediterranean water.* Rivista Italiana di Telerilevamento, 43 (3): 19-37. doi: http://dx.doi.org/10.5721/ItJRS20114332.

McClain C.R. (2009) - *A Decade of Satellite Ocean Color Observation*. Annual Review of Marine Science, 1: 19-42. doi: http://dx.doi.org/10.1146/annurev.marine.010908.163650.

Millot C. (1999) - *Circulation in the Western Mediterranean Sea*. Journal of Marine Systems, 20: 423-442. doi: http://dx.doi.org/10.1016/S0924-7963(98)00078-5.

Moore T.S., Campbell J.W., Dowell M.D. (2009) - *A class-based approach to characterizing and mapping the uncertainty of the MODIS ocean chlorophyll product.* Remote Sensing of Environment, 113: 2424-2430. doi: http://dx.doi.org/ 10.1016/j.rse.2009.07.016.

Morán X.A.G., Estrada M. (2001) - *Short-term variability of photosynthetic parameters and particulate and dissolved primary production in the Alboran Sea (SW Mediterranean)*. Marine Ecology Progress Series, 212: 53-67. doi: http://dx.doi.org/10.3354/meps212053.

Morel A., Prieur L. (1977) - *Analysis of variations in ocean color.* Limnology and Oceanography, 22 (4): 709-722. doi: http://dx.doi.org/10.4319/lo.1977.22.4.0709.

Morel A., Gentili B. (2009) - *The dissolved yellow substance and the shades of blue in the Mediterranean Sea*. Biogeosciences, 6: 2625-2636. doi: http://dx.doi.org/10.5194/bg-6-2625-2009.

Moulin C., Gordon H.R., Chomko R.M., Banzon V.F., Evans R.H. (2001) - *Atmospheric correction of ocean color imagery through thick layers of Saharan dust*. Geophysical Research Letters, 28 (1): 5-8. doi: http://dx.doi.org/10.1029/2000GL011803.

Navarro G., Alvain S., Vantrepotte V., Huertas I.E. (2014) - *Identification of dominant phytoplankton functional types in the Mediterranean Sea based on a regionalized remote sensing approach*. Remote Sensing of Environment, 152: 557-575. doi: http://dx.doi.org/10.1016/j.rse.2014.06.029.

O'Reilly J.E., Maritorena S., Mitchell B.G., Siegel D.A., Carder K.L., Garver S.A., Kahru M., McClain C. (1998) - *Ocean color chlorophyll algorithms for SeaWiFS.* Journal of Geophysical Research: Oceans, 103 (C11): 24937-24953. doi: http://dx.doi.org/10.1029/98JC02160.

O'Reilly J.E., Maritorena S., O'Brien M., Siegel D., Toole D., Menzies D., Smith R., Muelle J., Mitchell B., Kahru M., Chavez F., Strutton P., Cota G., Hooker S., McClain C., Carder K., Muller-Karger F., Harding L., Magnuson A., Phinney D., Moore G., Aiken J., Arrigo K., Letelier R., Culver M. (2000) - *Ocean color chlorophyll a algorithms for SeaWiFS, OC2, and OC4, Version 4.* In: SeaWiFS Postlaunch Calibration and Validation Analyses, Part 3, Hooker S.B., Firestone E.R. (Eds.), NASA Tech. Memo. 2000-206892, 11, NASA Goddard Space Flight Center, Greenbelt, Maryland, pp. 49.

Organelli E., Bricaud A., Antoine D., Matsuoka A. (2014) - *Seasonal dynamics of light absorption by chromophoric dissolved organic matter (CDOM) in the NW Mediterranean Sea (BOUSSOLE site)*. Deep-Sea Research I, 91: 72-85. doi: http://dx.doi.org/10.1016/j.dsr.2014.05.003.

Penna A., Bertozzini E., Battocchi C., Galluzzi L., Giacobbe M.G., Vila M., Garcés E., Lugliè A., Magnani M. (2007) - *Monitoring of HAB species in the Mediterranean Sea through molecular methods*. Journal Plankton Research, 29: 19-38. doi: http://dx.doi.org/10.1093/plankt/fbl053.

Robinson A.R., Leslie W.G., Theocharis A., Lascaratos A. (2001) - *Mediterranean Sea Circulation*. Encyclopedia of Ocean Sciences, Academic Press, 1689-1706. doi: http://dx.doi.org/10.1006/rwos.2001.0376.

Robinson W.D., Franz B.A., Patt F.S., Bailey S.W., Werdell P.J. (2003) - *Mask and Flags Updates*. In: Algorithm Updates for the Fourth SeaWiFS Data Reprocessing, Hooker S.B., Firestone E.R. (Eds.), 22 (6), NASA Technical Memorandum 2003-206892.

Santini C., Maselli F., Massi L., Pieri M. (2007) - *Applicazione di un modello ottico regionale per lo studio delle acque marine della Toscana*. Atti 11° Conferenza Nazionale ASITA,

Centro Congressi Lingotto, Torino 6-9 novembre 2007.

Santoleri R., Volpe G., Marullo S., Buongiorno Nardelli B. (2008) - *Observing the Mediterranean Sea from space: ocean colour algorithms and chlorophyll variability*. In: Remote Sensing of the European Seas, Barale V., Gade V.M. (Eds.), pp. 103-116. doi: http://dx.doi.org/10.1007/978-1-4020-6772-3_8.

Siegel D.A., Buesseler K.O., Doney S.C., Sailley S. F., Behrenfeld M.J., Boyd P.W. (2014) - *Global assessment of ocean carbon export by combining satellite observations and food-web models*. Global Biogeochemical Cycles, 28: 181-196. doi: http://dx.doi.org/10.1002/2013GB004743.

Siokou-Frangou I., Christaki U., Mazzocchi M.G., Montresor M., Ribera d'Alcalá M., Vaqué D., Zingone A. (2010) - *Plankton in the open Mediterranean Sea: a review*. Biogeosciences, 7: 1543-1586. doi: http://dx.doi.org/10.5194/bg-7-1543-2010.

Sohn Y., Rebello N.S. (2002) - *Supervised and unsupervised spectral angle classifiers.* Photogrammetric Engineering & Remote Sensing, 68 (12): 1271-1280.

Terauchi G., Tsujimoto R., Ishizaka J., Nakata H. (2014) - *Preliminary assessment of eutrophication by remotely sensed chlorophyll-a in Toyama Bay, the Sea of Japan.* Journal of Oceanograph, 70 (2): 175-184. doi: http://dx.doi.org/10.1007/s10872-014-0222-z.

Tilstone G.H., Peters S.W.M., Van der Woerd H.J., Eleveld M.A., Ruddick K., Schönfeld W., Krasemann H., Martinez-Vicente V., Blondeau-Patissier D., Röttgers R., Sørensen K., Jørgensen P.V., Shutler J.D. (2012) - *Variability in specific-absorption properties and their use in a semi-analytical ocean colour algorithm for MERIS in North Sea and Western English Channel Coastal Waters*. Remote Sensing of Environment, 118: 320-338. doi: http://dx.doi.org/10.1016/j.rse.2011.11.019.

Vidussi F., Claustre H., Bustillos-Guzmàn J., Cailliau C., Marty J.-C. (1996) - *Determination of chlorophylls and carotenoids of marine phytoplankton: separation of chlorophyll a from divinyl-chlorophyll a and zeaxanthin from letein.* Journal of Plankton Research, 18 (12): 2377-2382. doi: http://dx.doi.org/10.1093/plankt/ 18.12.2377.

Volpe G., Santoleri R., Vellucci V., Ribera d'Alcalà M., Marullo S., D'Ortenzio F. (2007) - *The colour of the Mediterranean Sea: Global versus regional bio-optical algorithms evaluation and implication for satellite chlorophyll estimates*. Remote Sensing of Environment, 107 (4): 625-638. doi: http://dx.doi.org/10.1016/j.rse.2006.10.017.

Volpe G., Colella S., Forneris V., Tronconi C., Santoleri R. (2012) - *The Mediterranean Ocean Colour Observing System - system development and product validation*. Ocean Science, 8: 869-883. doi: http://dx.doi.org/10.5194/os-8-869-2012.

Werdell P.J., Bailey S.W. (2005) - *An improved bio-optical data set for ocean color algorithm development and satellite data product validation.* Remote Sensing of Environment, 98 (1): 122-140. doi: http://dx.doi.org/10.1016/j.rse.2005.07.001.

Xiong X., Salomonson V.V., Barnes W.L., Chiang K., Erives H., Che N., Sun J. (2004) - *Status of Aqua MODIS on-orbit calibration and characterization*. Proceedings SPIE 5570, Sensors, Systems and Next-Generation Satellites VIII, 317 (November 4, 2004). doi: http://dx.doi.org/10.1117/12.564940.

Zibordi G., Mélin F., Voss K.J., Johnson B.C., Franz B.A., Kwiatkowska E., Huot J.-P., Wang M., Antoine D. (2015) - *System vicarious calibration for ocean color climate change applications: Requirements for in situ data*. Remote Sensing of Environment, 159: 361-369. doi: http://dx.doi.org/10.1016/j.rse.2014.12.015.